

This article was downloaded by:

On: 25 January 2011

Access details: *Access Details: Free Access*

Publisher *Taylor & Francis*

Informa Ltd Registered in England and Wales Registered Number: 1072954 Registered office: Mortimer House, 37-41 Mortimer Street, London W1T 3JH, UK



Liquid Crystals

Publication details, including instructions for authors and subscription information:

<http://www.informaworld.com/smpp/title~content=t713926090>

Dielectric studies of the nematic mixture E7 on a hydroxypropylcellulose substrate

M. T. Viciosa; A. M. Nunes; A. Fernandes; P. L. Almeida; M. H. Godinho; M. D. Dionísio

Online publication date: 11 November 2010

To cite this Article Viciosa, M. T. , Nunes, A. M. , Fernandes, A. , Almeida, P. L. , Godinho, M. H. and Dionísio, M. D.(2002) 'Dielectric studies of the nematic mixture E7 on a hydroxypropylcellulose substrate', *Liquid Crystals*, 29: 3, 429 – 441

To link to this Article: DOI: 10.1080/02678290110113478

URL: <http://dx.doi.org/10.1080/02678290110113478>

PLEASE SCROLL DOWN FOR ARTICLE

Full terms and conditions of use: <http://www.informaworld.com/terms-and-conditions-of-access.pdf>

This article may be used for research, teaching and private study purposes. Any substantial or systematic reproduction, re-distribution, re-selling, loan or sub-licensing, systematic supply or distribution in any form to anyone is expressly forbidden.

The publisher does not give any warranty express or implied or make any representation that the contents will be complete or accurate or up to date. The accuracy of any instructions, formulae and drug doses should be independently verified with primary sources. The publisher shall not be liable for any loss, actions, claims, proceedings, demand or costs or damages whatsoever or howsoever caused arising directly or indirectly in connection with or arising out of the use of this material.

Dielectric studies of the nematic mixture E7 on a hydroxypropylcellulose substrate

M. T. VICIOSA, A. M. NUNES, A. FERNANDES†, P. L. ALMEIDA‡, M. H. GODINHO‡ and M. D. DIONÍSIO*

Departamento de Química, Centro de Química Fina e Biotecnologia, Faculdade de Ciências e Tecnologia da Universidade Nova de Lisboa, 2825-114 Caparica, Portugal

†Centro de Química Estrutural da Universidade Técnica de Lisboa, Instituto Superior Técnico, Av. Rovisco Pais, 1049-001 Lisboa, Portugal

‡Departamento de Ciências do Materiais, Faculdade de Ciências e Tecnologia da Universidade Nova de Lisboa, 2825-114 Caparica, Portugal

(Received 12 March 2001; in final form 24 September 2001; accepted 10 October 2001)

To study the influence of a polymeric substrate, hydroxypropylcellulose (HPC), on the dynamics of the nematic mixture E7, the real (ϵ') and imaginary (ϵ'') parts of the complex dielectric permittivity of the unaligned composite system (polymeric substrate covered with liquid crystal) were measured as a function of frequency and temperature, and compared with those of unaligned pure E7. The temperature range was extended down to the supercooled region. Three superimposed processes were detected, related to different alignment states in relation to the electric field: (1) a main relaxation mechanism due to the hindered rotation of molecules about their short axis, corresponding to the case where the director is parallel to the electric field in an oriented sample, (2) a low frequency process attributed to molecular aggregates, and (3) a high frequency process due to the tumbling of molecules. Processes (2) and (3) correspond to the case when the director is perpendicular to the electric field in an oriented sample. In the composite system the main relaxation mechanism results in a faster process but the other two processes almost superimpose in the frequency window, the high frequency process being much more intense relative to pure E7. The enhancement of the high frequency process in HPC + E7 can be interpreted as an increase in the number of dipoles whose director has a component aligned perpendicular to the electric field, due to surface effects. The temperature dependence of the main and high frequency relaxation mechanisms obeys the VFT law, which is a feature of glass-like systems.

1. Introduction

The application of liquid crystals in display devices, due to their unusual electro-optic properties, has gained increasing interest in the past few years. Among these materials, special interest has been dedicated to polymer dispersed liquid crystals (PDLCs), i.e. low molecular mass liquid crystals randomly dispersed as microdroplets in a polymer film. Recently, Godinho *et al.* [1], introduced a new type of composite system produced from cellulose derivatives and a nematic mixture, E7, where a thin polymeric film of hydroxypropylcellulose (HPC) is placed between two nematic layers. This electro-optic cell reveals some advantages relative to usual PDLCs [2–4]. In the present work we intend to study the

molecular dynamics of E7 on the HPC substrate, as monitored by dielectric relaxation spectroscopy (DRS). This technique is sensitive to fluctuations of polarization that arise from reorientational motions of permanent dipoles resulting from the application of an electric field of oscillating low voltage (~ 1 V) to the material. In liquid crystal studies, dielectric relaxation spectroscopy gives information on the molecular dynamics via the anisotropic motions of the dipolar mesogenic units.

E7 is mainly a mixture of alkylcyanobiphenyls. The cyano end group is bonded to a rigid core of aromatic rings (see §2.1), providing a strong longitudinal dipole moment. Therefore DRS will probe mainly the motions of this strong dipole moment parallel to the molecular long axis.

In the literature, a high intensity absorption of the Debye type is described in the nematic phases of pure

*Author for correspondence

5CB and 7CB [5–9] (the main components of our nematic mixture). This is located in the low MHz region and is attributed to restricted rotation about the molecular short axis. This process was visible in experiments where the electric field was applied parallel to the nematic director [10], and is in accordance with the theory of Meier and Saupe. In the perpendicular geometry, a very broad and much less intense process, with a distribution of relaxation times, appears at higher frequencies [5, 7–10], and is attributed to the tumbling motion of the molecules. Nevertheless the interpretation of the molecular origin of this secondary process raises some doubts among different authors. If sufficiently detailed and accurate results over a large frequency range are available, it is possible to separate this process into several relaxation mechanisms (Martin *et al.* [11] demonstrated theoretically that this process corresponds to the superposition of several Debye processes). Bose *et al.* [12, 13] for 8CB, Wacrenier *et al.* [7] and Lippens *et al.* [6] resolved this broad process into three different relaxation domains between 10^7 and 10^9 Hz: a strong low frequency process due to the tumbling of molecules, and two weak mechanisms at higher frequencies. Following the results of Bose *et al.* [12, 13] (there is some agreement that the results of Wacrenier *et al.* [7] were probably caused by incomplete orientation of the sample [13, 14]), the two secondary processes are located around 225 and 600 MHz, and are temperature independent in the measured temperature range. The authors give two possible explanations for the origin of those peaks: persistence of a short range level of sufficient nematic order, or intramolecular motions of the molecules. Within the same frequency range and again for 7CB, Buka *et al.* [8] found only one broad relaxation process for the perpendicular alignment in relation to the electric field, with insufficient evidence of a reliable resolution. They also found two relaxation processes in the parallel alignment: a highly intense absorption process and a high frequency, low intensity process, located around 600 MHz, which is believed to arise from a relaxation process occurring within localized ordered regions.

All the dielectric relaxation phenomena described above are located in the megahertz and low gigahertz frequency ranges. Since the E7 nematic mixture under study supercools easily, it is our purpose to shift those high frequency processes observed for the pure components of E7 into our frequency window by measurements at lower temperatures.

By this work we hope to clarify the molecular motions underlying the relaxation processes accessible to our frequency range by studying pure E7, and to evaluate the variations of the molecular dynamics due to the interaction of E7 with the hydroxypropylcellulose substrate. While in the literature most studies are related to

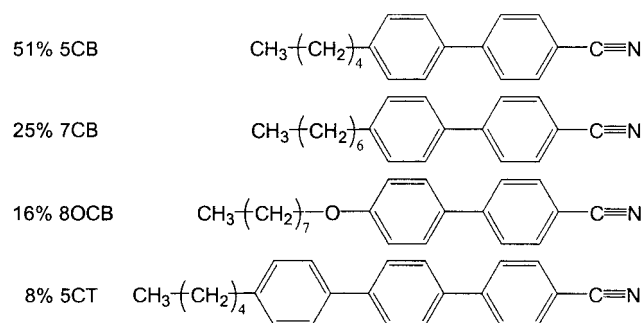
aligned samples, we will study unaligned samples, which means that the typical dielectric behaviour for both parallel and perpendicular alignments in the electric field in oriented samples can be found in our results.

Finally, due to the interface liquid crystal–polymer, an additional process arises; this is the Maxwell–Wagner effect, which is important in relation to studies of screening effects in the electro-optic cell.

2. Experimental

2.1. Materials and sample preparation

The nematic mixture E7 has the following composition [15, 16]:



Scheme. Structures of the components of the nematic liquid crystal mixture E7.

It was supplied by Merck and used as received. Solid films of about 30 μm thick were prepared from solutions of HPC (a commercial reagent grade from Aldrich, $M_w = 100\,000\text{ g mol}^{-1}$) and acetone (Pronalab), according to the method described previously [1]; prior to film preparation, the HPC powder was dried in vacuum at 50°C for about 48 h. Surface characterization by scanning electron microscopy (SEM) is described elsewhere [2]. The composite material was obtained by covering the rough surface of the solid film, with a 50 μm thick layer of the nematic mixture E7. The thickness of nematic E7 was controlled by two silica spacers (needle-shaped with a 50 μm cross section). The dielectric measurements were performed at least 24 h after the film was covered with the liquid crystal, to allow stabilization. This is the normal procedure used in electro-optical experiments [4]. When longer periods were used (we studied samples stabilized for 24 h, 48 h and 5 days), no visible changes were noticed in the dielectric results.

2.2. Dielectric relaxation spectroscopy

The dielectric measurements were performed on unaligned samples using a Hewlett-Packard impedance analyser HP 4284A, covering a frequency range from 20 Hz to 1 MHz. The temperature control was assured by a Quatro Cryosystem, manufactured by Novocontrol GmbH. The sample was placed between the two gold-plated electrodes (diameter 20 mm) of a parallel plate

capacitor; the C_0 (geometric capacitance of the cell) was 55.6 and 34.8 pF for, respectively, the pure E7 and HPC + E7 measurements. The sample cell (BDS 1200) was mounted on a cryostat (BDS 1100) and exposed to a heated gas stream evaporated from a liquid nitrogen Dewar, allowing temperature control with ± 0.02 K accuracy. Novocontrol supplied all these modules.

2.3. The fitting function

The Havriliak–Negami (HN) model function [17] was used for the data analysis. In the frequency domain the HN function reads:

$$\varepsilon^* = \varepsilon_\infty + \sum_j \frac{\Delta\varepsilon_j}{[1 + (i\omega/\omega_{oj})^{a_j}]^{b_j}} - i \frac{\sigma}{2\pi\varepsilon_0 f^c} \quad (1)$$

where j is the number of relaxation processes and $\omega_0 = 2\pi f_0$ is the characteristic HN frequency closely related with f_{\max} , the frequency of maximal loss; from this frequency a characteristic relaxation time $\tau = 1/(2\pi f_{\max})$ can be obtained, ε_∞ is the real permittivity for high frequencies compared with f_{\max} , i.e. $\varepsilon_\infty \cong \varepsilon'(f \gg f_{\max})$; $\Delta\varepsilon$ is the dielectric intensity or relaxation strength, measuring the difference in the real permittivity at low and high frequencies with respect to f_{\max} . The curve shape parameters a and b ($0 < a < 1$, $0 < ab < 1$) describe the slopes of the ε'' curve below and above the frequency of the peak: $a = \partial \log \varepsilon'' / \partial \log f$, for $f \ll f_0$, and $ab = -\partial \log \varepsilon'' / \partial \log f$ for $f \gg f_0$; the a value is related to the broadness of the relaxation, while b describes its asymmetry (Debye behaviour is given by $a = ab = 1$).

The dielectric data in the frequency domain were fitted by equation (1), and the fitting parameters are: $\Delta\varepsilon$, a , b , and τ . The conductivity contribution to the dielectric loss is given by the second term of equation (1), where ε_0 is the vacuum permittivity. σ and c are fitting parameters, σ being related to the d.c. conductivity of the sample, while c describes the broadening of the relaxation time distribution for the d.c. conductivity.

3. Results and discussion

E7 is a thermotropic liquid crystal mixture, with a quoted nematic range from $T_{C_{T \rightarrow N}} = 263$ K [15] to $T_{N \rightarrow I} = 333$ K, which easily forms a glassy nematic upon cooling and does not crystallize readily upon rewarming; it gives a glass transition at 211 K [15, 18, 19].

Dielectric relaxation spectra were collected in the range 293 to 213 K, covering the nematic (the first three dielectric loss curves) and the supercooled regions. The dielectric spectra were obtained with descending temperature steps of 1 K. At each temperature, the system was held for stabilization within ± 0.05 K. There is no discontinuity in the dielectric measurements at the quoted $T_{C_{T \rightarrow N}}$ of 263 K. The liquid crystal mixture was

also observed by polarizing optical microscopy while decreasing the temperature to 238 K. No evidence of crystallization was found in that temperature range.

In figure 1 we present the real (*a*) and the imaginary (*b*) parts of the complex dielectric constant for these spectra. The 3D plot of ε'' on a logarithmic scale is presented in figure 1(*c*).

We can observe a very high intensity absorption and, at high frequencies, a very broad and much less intense process—the logarithmic scale in figure 1(*c*) was chosen to resolve this second process better. From this figure the presence of a low frequency process partially merged in the high intensity peak is not clear. This low frequency process seems to be a true relaxation process as it cannot be fitted by conductivity, and the possibility of electrode polarization is ruled out since ε' does not show the usual increase at low frequencies characteristic of this type of polarization. In figure 2 we present the decomposition of the dielectric spectra at 236 K into the three different processes: the high intensity peak and the two secondary processes located at lower and higher frequencies relative to the main process.

The ε'' curves were fitted by equation (1); all the fitting parameters are listed in table 1. These parameters will be analysed further in the text.

The same experimental procedure was applied to obtain the relaxation spectra of the composite system of HPC film covered by a thin layer of E7. In addition to the dielectric loss curves obtained by cooling from 293 K, we also measured ε' and ε'' in the temperature range 293 to 373 K. In figure 3 we present, in linear (*a*), and in 3D logarithmic (*b*) scales, the imaginary part of the complex dielectric constant for this system (the real part will be presented in a later section).

Five relaxation processes are present in the HPC + E7 system from which three are observed in E7. These processes are: (1) a Maxwell–Wagner absorption at low frequencies and high temperatures due to the liquid crystal polymer interface; (2) the low frequency process (once more this process is not noticeable in the figure, but becomes evident during the fitting procedure as we have shown for pure E7); (3) the main relaxation process with a lower intensity than the same process in pure E7 (since the equivalent electrical circuit for the composite system is a series association of two different RC circuits, and due to the extremely low loss and capacitance values of the HPC film, the resulting capacitance and loss data for the composite system are significantly lower than the measured values for the pure liquid crystal); (4) the secondary process located at high frequencies, now more pronounced than it was for pure E7; and (5) a low intensity and broad process on the higher frequency side, for temperatures between 213 and 223 K, marked by an arrow in figure 3(*b*). We believe that this fifth

Table 1. Fitting parameters of the main and secondary relaxation processes of bulk E7 and HPC + E7.

| T/K | Main peak | | | | | | Secondary low frequency peak | | | | | | Secondary high frequency peak | | | | | | | | | | | | |
|------|--------------------|-------|-------|------------|--------------------|-------|------------------------------|------------|--------------------|----------|-------|------------|-------------------------------|-------|-------|------------|--------------------|-------|-------|------------|--------------------|-------|-------|------------|---|
| | E7 | | | HPC + E7 | | | E7 | | | HPC + E7 | | | E7 | | | HPC + E7 | | | | | | | | | |
| | $\Delta\epsilon_1$ | a_1 | b_1 | τ_1/s | $\Delta\epsilon_1$ | a_1 | b_1 | τ_1/s | $\Delta\epsilon_2$ | a_2 | b_2 | τ_2/s | $\Delta\epsilon_2$ | a_2 | b_2 | τ_2/s | $\Delta\epsilon_3$ | a_3 | b_3 | τ_3/s | $\Delta\epsilon_3$ | a_3 | b_3 | τ_3/s | |
| 271 | 16.01 | 0.96 | 1.00 | 1.12E-06 | 3.85 | 0.86 | 1.00 | 5.15E-07 | 1.50 | 0.73 | 0.78 | 2.77E-05 | 1.39 | 0.36 | 0.83 | 1.96E-05 | b | | | | b | | | | |
| 267 | 16.03 | 0.96 | 1.00 | 1.76E-06 | 3.79 | 0.87 | 1.00 | 8.28E-07 | 1.58 | 0.75 | 0.78 | 4.30E-05 | 1.31 | 0.38 | 0.85 | 2.66E-05 | b | | | | b | | | | |
| 263 | 15.90 | 0.96 | 1.00 | 2.82E-06 | 3.72 | 0.87 | 1.00 | 1.31E-06 | 1.63 | 0.73 | 0.84 | 6.50E-05 | 1.28 | 0.37 | 0.86 | 4.94E-05 | b | | | | b | | | | |
| 259 | 15.96 | 0.97 | 1.00 | 4.80E-06 | 3.69 | 0.87 | 1.00 | 2.15E-06 | 1.65 | 0.77 | 0.84 | 1.07E-04 | 1.25 | 0.38 | 0.88 | 7.47E-05 | b | | | | b | | | | |
| 255 | 16.14 | 0.97 | 1.00 | 8.45E-06 | 3.68 | 0.88 | 1.00 | 3.87E-06 | 1.60 | 0.79 | 0.82 | 1.83E-04 | 1.14 | 0.38 | 0.89 | 2.69E-04 | b | | | | b | | | | |
| 253 | 16.10 | 0.97 | 1.00 | 1.12E-05 | 3.64 | 0.88 | 1.00 | 5.13E-06 | 1.63 | 0.81 | 0.84 | 2.66E-04 | 1.10 | 0.40 | 0.90 | 3.05E-04 | a | | | | a | | | | |
| 252 | 16.11 | 0.97 | 1.00 | 1.36E-05 | 3.63 | 0.88 | 1.00 | 5.97E-06 | 1.62 | 0.75 | 0.76 | 3.99E-04 | 1.05 | 0.42 | 0.93 | 2.90E-04 | b | | | | b | | | | |
| 251 | 16.19 | 0.97 | 1.00 | 1.61E-05 | 3.66 | 0.88 | 1.00 | 7.19E-06 | 1.65 | 0.70 | 0.85 | 4.87E-04 | 0.95 | 0.45 | 0.95 | 5.32E-04 | b | | | | b | | | | |
| 250 | 16.13 | 0.97 | 1.00 | 1.91E-05 | 3.66 | 0.89 | 1.00 | 8.53E-06 | 1.65 | 0.72 | 0.78 | 6.32E-04 | 0.89 | 0.47 | 0.98 | 5.81E-04 | b | | | | b | | | | |
| 249 | 16.14 | 0.97 | 1.00 | 2.18E-05 | 3.64 | 0.89 | 1.00 | 1.02E-05 | 1.65 | 0.71 | 0.79 | 7.00E-04 | 0.90 | 0.47 | 0.99 | 8.42E-04 | b | | | | b | | | | |
| 248 | 16.14 | 0.98 | 1.00 | 2.68E-05 | 3.63 | 0.89 | 1.00 | 1.21E-05 | 1.60 | 0.74 | 0.81 | 9.47E-04 | 0.88 | 0.48 | 0.99 | 8.40E-04 | 0.19 | 0.67 | 0.78 | 1.89E-07 | 1.08 | 0.99 | 0.28 | 3.05E-07 | |
| 247 | 16.14 | 0.98 | 1.00 | 3.18E-05 | 3.62 | 0.90 | 0.98 | 1.45E-05 | 1.63 | 0.75 | 0.82 | 1.04E-03 | 0.87 | 0.49 | 0.99 | 8.18E-04 | 0.22 | 0.67 | 0.79 | 1.97E-07 | 1.08 | 1.00 | 0.29 | 3.31E-07 | |
| 246 | 16.11 | 0.98 | 1.00 | 3.79E-05 | 3.68 | 0.89 | 1.00 | 1.72E-05 | 1.60 | 0.77 | 0.84 | 1.19E-03 | 0.72 | 0.54 | 0.98 | 1.22E-03 | 0.24 | 0.66 | 0.77 | 3.14E-07 | 1.09 | 0.98 | 0.30 | 3.72E-07 | |
| 245 | 16.09 | 0.99 | 1.00 | 4.51E-05 | 3.67 | 0.89 | 1.00 | 2.07E-05 | 1.58 | 0.85 | 0.89 | 1.30E-03 | 0.70 | 0.54 | 0.99 | 1.32E-03 | 0.26 | 0.66 | 0.79 | 3.65E-07 | 1.09 | 0.97 | 0.31 | 4.19E-07 | |
| 244 | 16.09 | 0.99 | 1.00 | 5.41E-05 | 3.67 | 0.89 | 1.00 | 2.52E-05 | 1.55 | 0.81 | 0.87 | 1.35E-03 | 0.61 | 0.60 | 1.00 | 1.63E-03 | 0.28 | 0.67 | 0.79 | 3.72E-07 | 1.09 | 0.96 | 0.32 | 4.93E-07 | |
| 243 | 15.91 | 0.99 | 1.00 | 6.55E-05 | 3.65 | 0.90 | 1.00 | 3.06E-05 | 1.58 | 0.85 | 0.89 | 1.82E-03 | 0.60 | 0.62 | 1.00 | 1.87E-03 | 0.30 | 0.66 | 0.73 | 3.62E-07 | 1.08 | 0.94 | 0.33 | 6.32E-07 | |
| 242 | 15.90 | 0.99 | 1.00 | 7.90E-05 | 3.63 | 0.90 | 1.00 | 3.66E-05 | 1.58 | 0.86 | 0.89 | 1.86E-03 | 0.59 | 0.63 | 1.00 | 1.85E-03 | 0.31 | 0.66 | 0.72 | 3.87E-07 | 1.08 | 0.94 | 0.34 | 7.06E-07 | |
| 241 | 15.73 | 0.99 | 1.00 | 9.65E-05 | 3.59 | 0.90 | 1.00 | 4.40E-05 | 1.53 | 0.88 | 0.90 | 1.94E-03 | 0.58 | 0.64 | 1.00 | 1.93E-03 | 0.32 | 0.66 | 0.71 | 5.81E-07 | 1.08 | 0.96 | 0.32 | 8.81E-07 | |
| 240 | 15.70 | 0.99 | 1.00 | 1.18E-04 | 3.54 | 0.91 | 1.00 | 5.41E-05 | 1.53 | 0.90 | 0.91 | 2.05E-03 | 0.58 | 0.64 | 0.94 | 1.95E-03 | 0.32 | 0.66 | 0.72 | 6.19E-07 | 1.06 | 0.96 | 0.33 | 1.07E-06 | |
| 239 | 15.61 | 1.00 | 1.00 | 1.45E-04 | 3.48 | 0.91 | 1.00 | 6.75E-05 | 1.65 | 0.91 | 0.91 | 2.10E-03 | 0.56 | 0.64 | 0.99 | 2.01E-03 | 0.33 | 0.65 | 0.73 | 8.29E-07 | 1.05 | 0.95 | 0.34 | 1.31E-06 | |
| 238 | 15.21 | 1.00 | 1.00 | 1.81E-04 | 3.47 | 0.91 | 1.00 | 8.43E-05 | 1.70 | 0.91 | 0.91 | 2.25E-03 | 0.52 | 0.65 | 1.00 | 2.06E-03 | 0.34 | 0.66 | 0.72 | 1.25E-06 | 1.03 | 0.96 | 0.34 | 1.62E-06 | |
| 237 | 15.05 | 1.00 | 1.00 | 2.24E-04 | 3.43 | 0.91 | 1.00 | 1.05E-04 | a | | | | 0.51 | 0.65 | 1.00 | 2.50E-03 | 0.36 | 0.65 | 0.76 | 1.97E-06 | 1.02 | 0.95 | 0.36 | 1.96E-06 | |
| 236 | 15.05 | 1.00 | 1.00 | 2.84E-04 | 3.55 | 0.90 | 1.00 | 1.38E-04 | a | | | | a | | | | 0.35 | 0.66 | 0.75 | 2.02E-06 | 1.03 | 0.94 | 0.37 | 2.49E-06 | |
| 235 | 15.04 | 1.00 | 1.00 | 3.60E-04 | 3.51 | 0.90 | 1.00 | 1.78E-04 | a | | | | a | | | | 0.35 | 0.66 | 0.76 | 2.67E-06 | 1.02 | 0.95 | 0.36 | 3.22E-06 | |
| 234 | 14.80 | 1.00 | 1.00 | 4.72E-04 | 3.47 | 0.90 | 1.00 | 2.30E-04 | a | | | | a | | | | 0.38 | 0.66 | 0.78 | 3.94E-06 | 1.03 | 0.96 | 0.35 | 4.25E-06 | |
| 233 | 14.85 | 1.00 | 1.00 | 6.17E-04 | 3.38 | 0.90 | 1.00 | 3.06E-04 | a | | | | a | | | | 0.38 | 0.66 | 0.78 | 4.83E-06 | 1.06 | 0.94 | 0.35 | 5.87E-06 | |
| 232 | 14.83 | 1.00 | 1.00 | 8.18E-04 | 3.28 | 0.90 | 1.00 | 4.01E-04 | a | | | | a | | | | 0.39 | 0.68 | 0.79 | 6.27E-06 | 1.06 | 0.94 | 0.36 | 7.79E-06 | |
| 231 | 14.31 | 1.00 | 1.00 | 1.08E-03 | 3.24 | 0.90 | 1.00 | 5.27E-04 | a | | | | a | | | | 0.42 | 0.68 | 0.77 | 8.65E-06 | 1.06 | 0.94 | 0.36 | 1.04E-05 | |
| 230 | 14.05 | 0.99 | 1.00 | 1.50E-03 | 3.17 | 0.89 | 1.00 | 7.21E-04 | b | | | | b | | | | 0.44 | 0.69 | 0.77 | 1.30E-05 | 1.07 | 0.95 | 0.34 | 1.47E-05 | |
| 229 | 13.66 | 1.00 | 1.00 | 1.97E-03 | 3.04 | 0.90 | 1.00 | 9.63E-04 | b | | | | b | | | | 0.47 | 0.69 | 0.81 | 1.42E-05 | 1.11 | 0.94 | 0.34 | 2.21E-05 | |
| 228 | 13.18 | 0.99 | 1.00 | 2.68E-03 | 2.96 | 0.91 | 0.98 | 1.33E-03 | b | | | | b | | | | 0.48 | 0.70 | 0.80 | 1.89E-05 | 1.11 | 0.95 | 0.33 | 3.05E-05 | |
| 227 | 12.85 | 0.98 | 1.00 | 3.81E-03 | 2.85 | 0.95 | 0.88 | 2.06E-03 | b | | | | b | | | | 0.50 | 0.69 | 0.82 | 2.46E-05 | 1.10 | 0.95 | 0.31 | 4.57E-05 | |
| % | 1-6 | 1-3 | 1 | 2-8 | 2-4 | 6 | 1-2 | 2-10 | | | 10 | | | | 10 | | | | | 10 | | 1-2 | 3-4 | 10 | 3 |
| unc. | | | | | | | | | | | | | | | | | | | | | | | | | |

^a Insufficient data to allow a reliable fitting.

^b Peak out of frequency range.

^c Uncertainty affecting the fitting parameters.

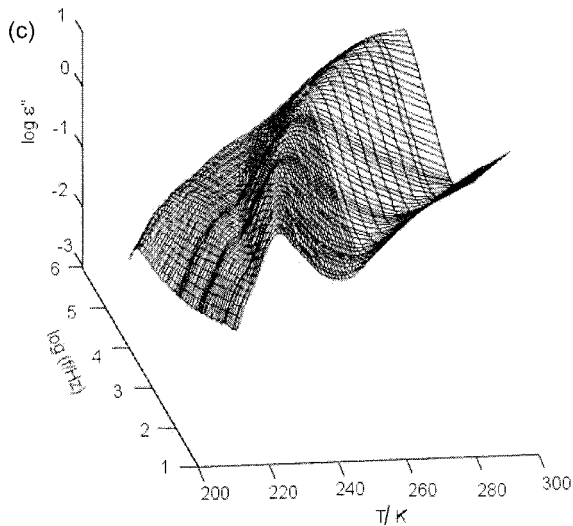
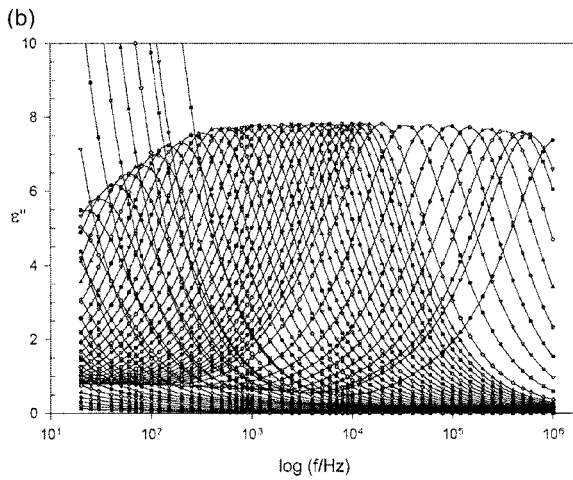
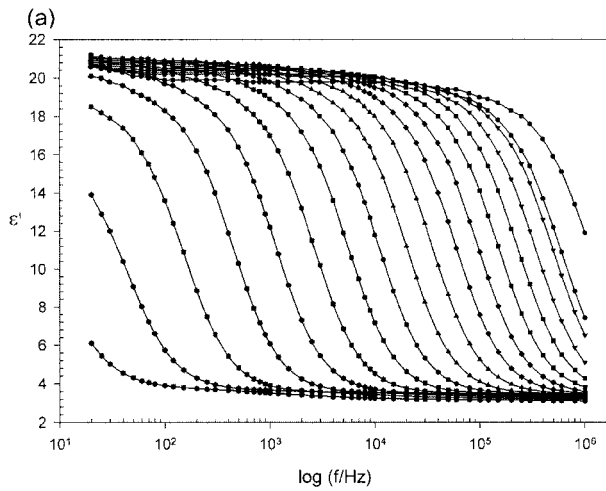


Figure 1. The complex dielectric constant of pure E7 measured between 213 and 293 K: (a) the real part in 4 K temperature steps, (b) the imaginary part in steps varying from 4 to 1 K, (c) the 3D representation with ε'' on a logarithmic scale.

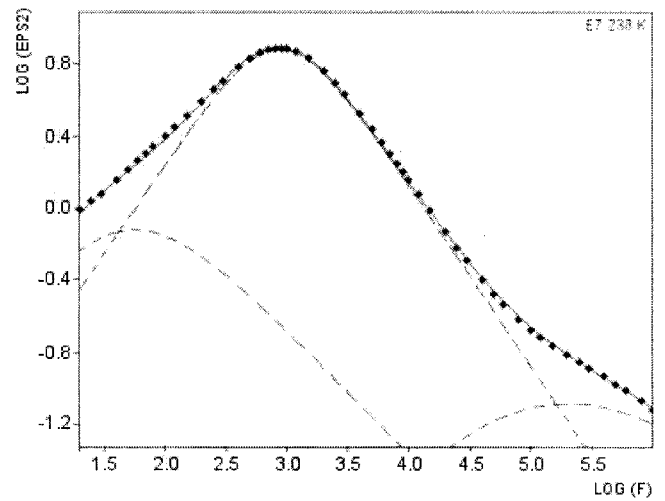


Figure 2. Dielectric loss curve for bulk E7 at 238 K. Filled squares: experiment; solid line: fitting which is a superposition of the three relaxation processes described (dashed lines).

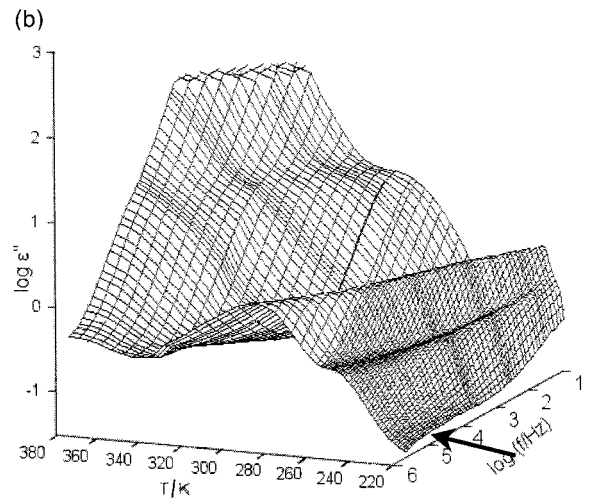
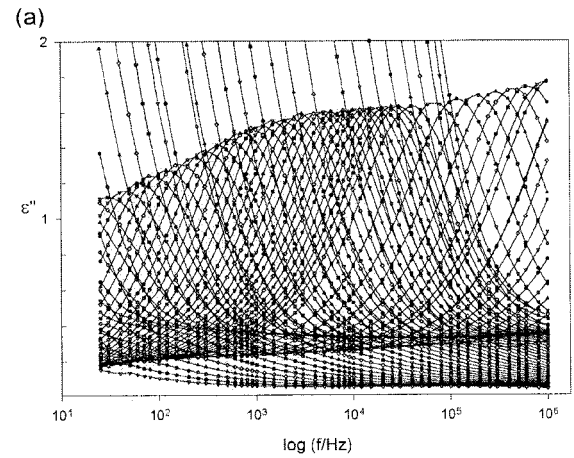


Figure 3. Dielectric loss curves of HPC+E7 between 213 and 373 K (a) on a linear scale (b) in a 3D representation with ε'' on a logarithmic scale.

relaxation is due to the hydroxypropylcellulose substrate itself. In figure 4 we present the relaxation spectra for the HPC film, with a very broad and low intensity process on the high frequency side. Increasing the temperature, the relaxation spectra of the polymer film itself are no longer noticeable in the composite system, since their intensity is very low compared with the increasing intensity of the overall dielectric spectra.

The dielectric data for the composite system were also fitted by equation (1) and the fitting parameters are included in table 1. From here on, to be clearer, we will analyse separately the main and the secondary processes observed in both E7 and HPC + E7 systems.

3.1. The main relaxation process

The main relaxation process is largely a single time process, at least for pure E7. The shape parameters a , b listed in table 1 reveal a Debye relaxation function which is characterized by $a = 1$ and $b = 1$ in equation (1). In the composite system the loss peak maintains its symmetry ($b = 1$ for the whole temperature range), but the a parameter decreases to 0.89 ± 0.02 , which implies some distribution of relaxation times.

The dielectric strength of the main relaxation process, $\Delta\epsilon_1$, obtained in the HN fits for both systems, remains almost unchanged over a large temperature range, but there is a critical temperature below which a pronounced decrease of the dielectric strength (and ϵ''_{\max}) occurs. We will analyse this behaviour further in the text.

The relaxation times obtained for the main relaxation process from the HN fittings, for both E7 and HPC + E7, are plotted against the reciprocal of temperature in figure 5.

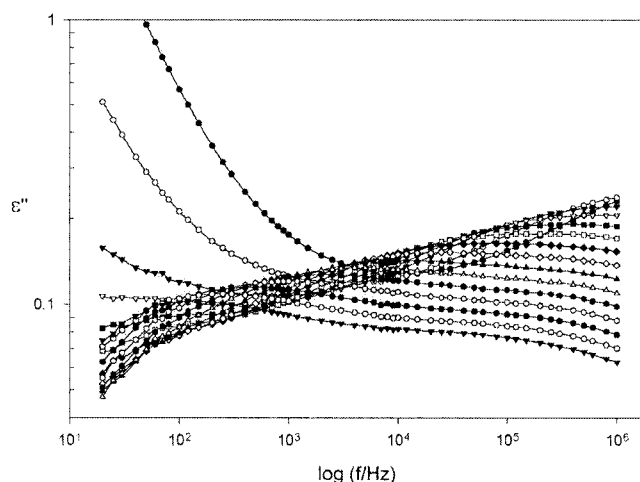


Figure 4. Dielectric loss curves of HPC film in the temperature range from 213 and 293 K in 5 K temperature steps.

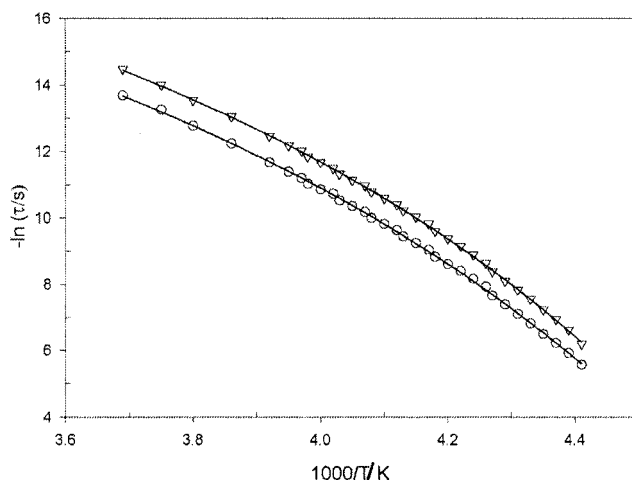


Figure 5. Activation plot of the temperature dependence of the relaxation times for the main relaxation process for bulk E7 (circles) and HPC + E7 (triangles). Solid lines: VFT fits.

The curvature affecting the temperature dependence of the relaxation times obeys the Vogel–Fulcher–Tamman law:

$$\tau = \tau_0 \exp[B/(T - T_0)] \quad (2)$$

with the following parameters: $\tau_0 = (1.7 \pm 0.5) \times 10^{-11}$ s, $B = 1168 \pm 52$ K and $T_0 = 165.9 \pm 1.7$ K for E7, and $\tau_0 = (1.5 \pm 0.4) \times 10^{-11}$ s, $B = 1058 \pm 40$ K and $T_0 = 170.1 \pm 1.3$ K for HPC + E7. The T_0 values are 45 and 41 K lower, respectively for E7 and HPC + E7, than the calorimetric T_g value of pure E7, as would be expected for this parameter in the VFT equation; usually T_0 is about 30–50 K lower than the calorimetric T_g , suggesting that the glass transition temperature of E7 in the composite system is about 4 K higher than the T_g of pure E7.

In the literature, the peaks for the relaxation mechanism due to the hindered rotation about the molecular short axis, found in oriented samples in the case where the director is parallel to the electric field, are symmetrical and the temperature dependence in the bulk nematic phase of the relaxation times is Arrhenian. However, this is not the case in supercooled liquid crystals. The activation plots of the main process attributed to the reorientations of molecules around their short axes in confined 5CB [20, 21] and 8CB [21] in the supercooled state show some curvature. Also Zeller [22] found VFT behaviour in several supercooled nematics confirming the universality of the VFT law in glass-forming systems. By replacing equation (2) in the apparent activation energy equation:

$$Q_{\text{app}} = R \frac{\partial \ln \tau}{\partial (1/T)} \quad (3)$$

it is possible to calculate a temperature dependent activation energy, equation (4).

$$Q_{\text{app}}(T) = \frac{R.B}{\left(1 - \frac{T_0}{T}\right)^2}. \quad (4)$$

The VFT parameters determined above were replaced in equation (4) and the activation energies calculated. The values obtained for E7 and HPC + E7 are listed in table 2, increasing from 64 kJ mol⁻¹ (at 271 K) to around 140 kJ mol⁻¹ (at 227 K). The values of Q_{app} agree for both systems within their uncertainties.

There is some agreement between the values of the activation energies for the mechanism involving the

hindered rotations of molecules around their short axes in oriented samples in the parallel geometry, for several liquid crystals with similar structures; the values are around 50–70 kJ mol⁻¹ [8, 23–25]. These activation energy values agree with the behaviour of our liquid crystal in the high temperature region, in the nematic range (see Q_{app} in table 2 for $T \geq 263$ K). Below that temperature, the activation energy increases with decreasing temperature as in a glass-forming liquid, and the temperature dependence becomes non-Arrhenian. This behaviour can be explained in terms of the potential energy landscape, since the regions of the potential energy surface or landscape that a liquid explores depends on temperature. The potential energy surface contains a number of local minima, termed ‘inherent structures’ by Stillinger and Weber [26], each of which is surrounded by a ‘basin’ which is defined such that a local minimization of the potential energy maps any point in the basin to the inherent structure contained within it. The time evolution of a liquid may be viewed as a succession of transitions from one basin to another occurring differently with temperature [27]. With the proximity of the glass transition, the system has to overcome higher energy barriers between those minima, this being the reason why the activation energy increases with decreasing temperature.

Our activation energy values are in accordance with Zhong *et al.* [15], who determined an activation energy value of 100 kJ mol⁻¹ independent of the alignment state of the nematic director in the electric field. They also found VFT behaviour for the main dielectric relaxation process in the E7 liquid crystal mixture, attributing this to the rotations of the longitudinal components of the dipole moments about their short axes. These authors studied the relaxation of E7 dispersed in PMMA (a PDLC system). Some of our observations agree with the 50% E7/PMMA system studied. In that system the relaxation frequency of the loss peaks deviates in a constant manner, higher by 0.5 decade, or on a temperature scale, lower by 5 K than for pure E7. In our composite system there is also a constant deviation to higher frequencies of the location of the maximum of the loss peaks relative to pure E7, by 0.3 decade (see last column in table 2). On a temperature scale, the peaks of the composite system deviate between 3 and 4 K to lower temperatures, relative to pure E7, i.e. in the composite system, the liquid crystal anticipates in temperature its pure behaviour.

We conclude that the mobility of the main relaxation mechanism of the liquid crystal increases, i.e. the rotational fluctuations of the molecules around their short molecular axes are faster when the liquid crystal relaxes on the hydroxypropylcellulose substrate.

Table 2. Apparent activation energies of the main relaxation process for bulk E7 and HPC + E7, calculated using the VFT parameters (see text); frequency position (in decades of frequency) of the maximum of the peak for the main relaxation process of both systems and the respective difference—distance between main peaks in decades of frequency.

| T/K | Q_{app} (kJ.mol ⁻¹) | | $\log_{10} f$ | | |
|-----|--|----------|---------------|----------|----------------------|
| | E7 | HPC + E7 | E7 | HPC + E7 | $\Delta \log_{10} f$ |
| 271 | 65 ± 5 | 64 ± 4 | 5.2 | 5.5 | 0.3 |
| 267 | 68 ± 5 | 67 ± 4 | 5.0 | 5.3 | 0.3 |
| 263 | 71 ± 6 | 71 ± 5 | 4.8 | 5.1 | 0.3 |
| 259 | 75 ± 6 | 75 ± 5 | 4.5 | 4.9 | 0.3 |
| 255 | 80 ± 7 | 80 ± 5 | 4.3 | 4.6 | 0.3 |
| 253 | 82 ± 7 | 82 ± 6 | 4.2 | 4.5 | 0.3 |
| 252 | 83 ± 7 | 83 ± 6 | 4.1 | 4.4 | 0.4 |
| 251 | 85 ± 7 | 85 ± 6 | 4.0 | 4.3 | 0.4 |
| 250 | 86 ± 7 | 86 ± 6 | 3.9 | 4.3 | 0.3 |
| 249 | 87 ± 7 | 88 ± 6 | 3.9 | 4.2 | 0.3 |
| 248 | 89 ± 8 | 89 ± 6 | 3.8 | 4.1 | 0.3 |
| 247 | 90 ± 8 | 91 ± 7 | 3.7 | 4.0 | 0.3 |
| 246 | 92 ± 8 | 93 ± 7 | 3.6 | 4.0 | 0.3 |
| 245 | 93 ± 8 | 94 ± 7 | 3.5 | 3.9 | 0.3 |
| 244 | 95 ± 8 | 96 ± 7 | 3.5 | 3.8 | 0.3 |
| 243 | 97 ± 9 | 98 ± 7 | 3.4 | 3.7 | 0.3 |
| 242 | 99 ± 9 | 100 ± 7 | 3.3 | 3.6 | 0.3 |
| 241 | 100 ± 9 | 102 ± 8 | 3.2 | 3.6 | 0.3 |
| 240 | 102 ± 9 | 104 ± 8 | 3.1 | 3.5 | 0.3 |
| 239 | 104 ± 9 | 106 ± 8 | 3.0 | 3.4 | 0.3 |
| 238 | 106 ± 10 | 108 ± 8 | 2.9 | 3.3 | 0.3 |
| 237 | 108 ± 10 | 111 ± 8 | 2.9 | 3.2 | 0.3 |
| 236 | 110 ± 10 | 113 ± 9 | 2.7 | 3.1 | 0.3 |
| 235 | 113 ± 11 | 116 ± 9 | 2.6 | 3.0 | 0.3 |
| 234 | 115 ± 11 | 118 ± 9 | 2.5 | 2.8 | 0.3 |
| 233 | 118 ± 11 | 121 ± 10 | 2.4 | 2.7 | 0.3 |
| 232 | 120 ± 11 | 124 ± 10 | 2.3 | 2.6 | 0.3 |
| 231 | 123 ± 12 | 127 ± 10 | 2.2 | 2.5 | 0.3 |
| 230 | 126 ± 12 | 130 ± 11 | 2.0 | 2.3 | 0.3 |
| 229 | 128 ± 13 | 133 ± 11 | 1.9 | 2.2 | 0.3 |
| 228 | 132 ± 13 | 137 ± 11 | 1.8 | 2.1 | 0.3 |
| 227 | 135 ± 13 | 140 ± 12 | 1.6 | 1.9 | 0.3 |

3.2. The secondary relaxations

The fitting parameters of the secondary peaks for both systems E7 and HPC+ E7 are included in table 1. In the composite system, the dielectric strength of the high frequency process is higher than in pure E7, which facilitates the fitting procedure (note that, at each temperature, the uncertainty that affects the fitting parameters is lower than the uncertainty for the same peak in pure E7—last row in table 1).

In figure 6 we present the temperature dependence of the relaxation times for the two secondary processes in both systems. There is a remarkable accordance between the data from the two different systems, in spite of the difficulty in performing the fittings of the low frequency secondary process in both systems, and of the high frequency process in E7.

The activation plot of the high frequency peak for both systems presents some curvature. This behaviour is closely followed by the low frequency process, with the exception of the lowest temperatures where the location of the loss peak seems to remain unchanged for both E7 and HPC+ E7. We will interpret this temperature dependence further in the text.

The question that we ask ourselves is ‘what mechanism is involved in these secondary processes?’ An explanation for the high frequency peak could be the internal rotation of the oxy (—O—) group of 8OCB. However, dielectric relaxation studies on alkoxy cyanobiphenyls have revealed no evidence of a relaxation process due to the internal rotation of the oxy group [8, 28].

Since we are studying a mixture of liquid crystals, can these secondary peaks be due to the different components of the mixture? In nematic mixtures of chemically similar

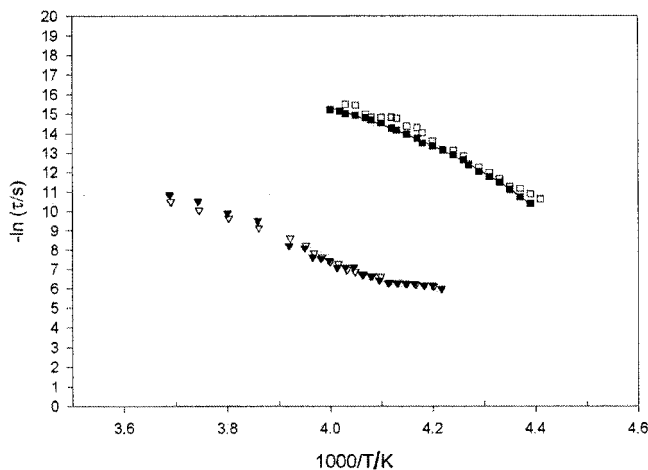


Figure 6. Activation plot of the temperature dependence of the relaxation times for the two secondary processes for bulk E7 (open symbols) and HPC+ E7 (filled symbols). Squares: high frequency process; triangles: low frequency process.

compounds, like the 5CB and 7CB components [29], a single peak is observed showing a collective behaviour due to the nematic potential. In order to clarify the distinction between collective behaviour and single-particle behaviour, Zeller [22, 24] studies a supercooled mixture of 5CB and 5CT, of which the latter component differs in the length of the rigid part: 5CB is a biphenyl while 5CT is a terphenyl. This author found single-particle behaviour in this binary mixture, i.e. two relaxation processes were observed for parallel alignment. The high frequency was attributed to the binuclear compound 5CB, and the slow process to the trinuclear compound 5CT. Since in our mixture the concentration of 5CB is 51% while that of 5CT is only 8%, if single particle behaviour were observed, then the main peak should be attributed to 5CB and the low frequency peak to 5CT. Zeller found an increasing deviation with decreasing temperature between the maxima of the peaks corresponding to each compound, due to different activation energies of the individual components. In our case, the difference in frequency between the maximum of the main peak and the maximum of the low frequency peak in pure E7 is approximately constant and equal to 1.4 decades over almost all the temperature range; this means that the peaks move concomitantly—only at the lowest temperatures (241–238 K), does the difference decrease to 1.1 decades due to the unchanged position of the low frequency peak.

Being aware that Zeller's observations were found for parallel aligned samples, we still have some doubts that the single particle explanation applies to our case. The possibility of resolving our dielectric curves into several single particle mechanisms is weakened when we compare the location of the dielectric loss peaks of the secondary processes between the two systems: the location in a frequency or temperature window does not change, and only the intensity is altered. If a specific interaction between one of the components of the nematic mixture develops when E7 rests on hydroxypropyl-cellulose—for instance, we can conceive of some interaction between the cellulosic groups of the polymer matrix and the oxy group of 8OCB—then the peak intensity could change as we observe; but certainly a deviation of the maximum loss would occur relative to pure E7 (modification of the relaxation times), which is not the case. On the other hand, if the secondary peaks are due to individual components with no specific interactions with the polymeric matrix, there is no reason to modify their relative intensities in relation to pure E7, as happens in the composite system: the relative weight of both $\Delta\epsilon_2$ and $\Delta\epsilon_3$ (respectively, the dielectric strengths of the low and high frequency processes) relative to the main process, is greatly increased in the composite system. Moreover, the activation energies will be different

(Zeller [22, 24] found different activation energies for 5CB and 5CT), leading to different separations between the peaks with temperature variation, which does not apply to our findings. In conclusion, we are convinced that this mixture presents the behaviour of a single component unaligned liquid crystal, whereby we expect to observe the typical dielectric behaviour of both parallel and perpendicular alignments of the nematic director in the electric field found in oriented samples. The work of Schönhalz *et al.* [30] with unaligned 8CB is an example of the expected behaviour where both the main relaxation and high frequency processes were detected in dielectric measurements. The first was assigned to rotational fluctuations of molecules around the short axis, corresponding to the case when the director is aligned parallel to the electric field; the high frequency process is attributed to the case when the director is aligned perpendicular to the electric field. The experiments described in the next section will help to confirm that an identical behaviour could be found in our liquid crystal mixture.

3.3. Fast cooling experiments

As mentioned before, there is a critical temperature below which both ϵ_{max}^n and $\Delta\epsilon$ of the main process begin to decrease markedly; this behaviour was also reported by Zeller [15] for pure E7. In figure 7 we show, for both systems, the dielectric strength of the main process, $\Delta\epsilon_1$, as a function of the temperature (on a logarithmic scale to emphasize the variation of slope). The abrupt change occurs at 233 K for E7 and 236 K for HPC + E7.

A DSC transition close to these temperature values (244 K), is reported by Manaila-Maximean *et al.* [31] for pure E7. In a preliminary study we also observed a

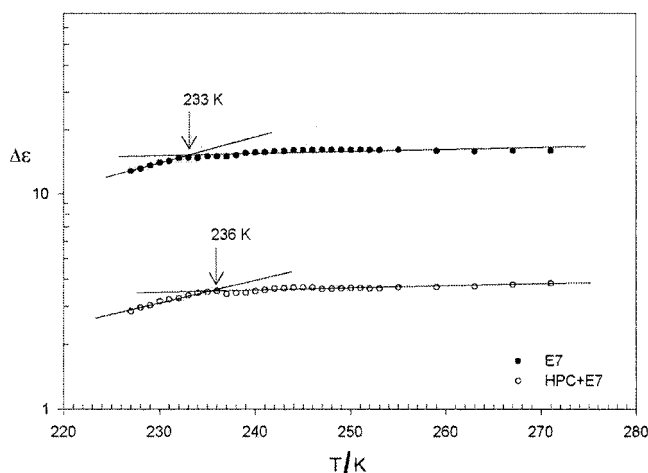


Figure 7. Temperature dependence of the dielectric strength of the main relaxation process on a logarithmic scale (the lines are guides for the eye). Filled circles: bulk E7; open circles: HPC + E7.

transition by DSC around 248 K, but more studies are in progress in order to evaluate its reproducibility and to clarify its nature (see figure 8).

In view of this behaviour we performed a different type of experiment. The sample was cooled directly from 293 K at a rate of about -7 K min^{-1} , down to a preset temperature above and below the critical temperature where the dielectric strength decreases abruptly, and the dielectric spectra were collected immediately after the temperature was reached (with a stabilization within $\pm 0.1 \text{ K}$). The loss curves obtained by these fast cooling experiments overlap the loss curves obtained in the normal cooling experiments for temperatures 10 K higher than 233 K and 236 K for E7 and HPC + E7, respectively. However, for temperatures slightly higher or lower than those values, the heights of the dielectric peaks change markedly: for both systems, there is an enhancement of both the low and high frequency processes and a decrease of the main process.

Additionally, we measured the dielectric spectra after keeping the sample at the same temperature for 30 min. In figure 9 we present the imaginary part of the complex dielectric constant obtained at 237 K after a fast cooling, together with the curve obtained 30 min later (the sample was kept at 237 K), for (a) pure E7 and (b) the composite system, and the curve obtained during the normal cooling experiments. The figure clearly shows that the curves obtained after 30 min at 237 K following the fast cooling, tend to superpose those obtained in the normal cooling experiments.

These observations indicate a time dependent behaviour: we are cooling an anisotropic liquid crystalline phase where the molecular orientations are changing on a time scale within the time scale of the experiment. These fast cooling experiments lead us to think that there is some exchange between the different relaxation processes, i.e. if a partial quantity of the dipole moment vector associated with each process relaxes, then a decrease in $\Delta\epsilon$ of the main process should correspond to a complementary increase in $\Delta\epsilon$ of the secondary processes; on aging the sample for 30 min at the same low temperature, the dielectric strength partially or fully recovers (a complete report of these experimental results with quantitative analysis of the data, together with ongoing DSC studies, will be published in the future).

The previously described experiments allow us to confirm that the observed relaxation processes are related to dipole alignments. Either in the normal cooling or fast cooling experiments, there is an increase in the intensity of the high frequency relaxation process in HPC + E7 relative to pure E7. This high frequency process should be related to the tumbling motion of the molecules, i.e. the fluctuations of the dipole moment along the molecular long axis, around the local director, found in

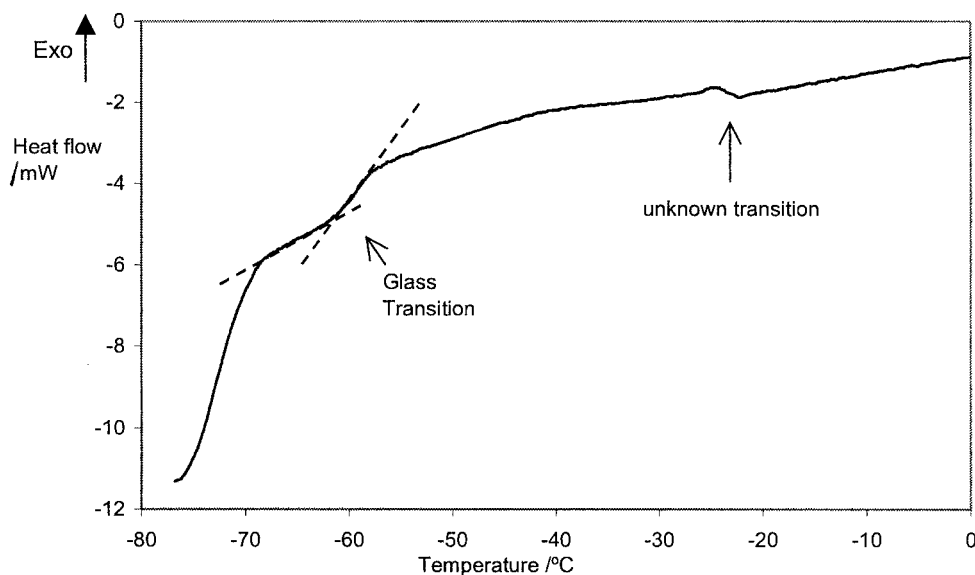


Figure 8. Thermogram of pure E7 obtained using a Setaram DSC 121, with a heating rate of $1^{\circ}\text{C min}^{-1}$ after the sample has been cooled to -8°C at $1^{\circ}\text{C min}^{-1}$. During the experiments the sample holder was continuously purged with argon.

oriented samples where the nematic director is aligned normal to the electric field. This enhancement of the high frequency process in the composite system can be due either to an increase in the number of dipoles whose director has a component aligned perpendicular to the electric field, or to a greater amplitude of the fluctuations of the long molecular axis in this tumbling mechanism which will decrease the relaxation rate [23]. In our study, and since the relaxation time of this high frequency process does not change when the E7 is relaxing on the HPC film, we can simply assume an increase in the number of dipole moment vectors with a component along the direction normal to the electric field, due to surface effects. This behaviour seems to be in accord with electro-optical results in different HPC + E7 cells [32] where it is concluded that the voltage, at 1 kHz, necessary to switch the cells to the transparent state, V_{on} (see next section), is mainly determined by liquid crystal polymer surface interactions and corresponds to the voltage necessary to reorient the director in the layers of the nematic close to the polymer surface. The increase in the V_{on} value relative to the pure E7 observed in these studies indicates, besides the low dielectric constant of the film, that the interactions with the polymeric film lead to a strong alignment of the director along the film surface with a distribution of orientations in the plane of the surface.

The high frequency relaxation is found to be temperature dependent in both pure E7 and HPC + E7, contrary to the observed temperature independence in pure bulk liquid crystals. Nevertheless, Nazario *et al.* [23] found, in 5CB confined in 2000 Å cylindrical pores in

the supercooled state, a temperature dependence of the librational (tumbling) mode, mainly determined by viscosity, which presents some curvature in the plot $\ln(\tau)$ vs $1/T$. The same behaviour was found by Cramer *et al.* [20] in 5CB in a different pore dimension (5 nm): the process due to the libration (or tumbling) of molecules (process Ia according to the authors) presents curvature in the plot $\log(1/\tau_{max})$ vs $1/T$ in the supercooled state, and the curve closely follows the temperature dependence of the main relaxation process. Therefore our findings are in accord with the results obtained by those authors for the supercooled state.

The low frequency secondary process is due probably to molecular aggregates, since it is a relaxation mechanism with a longer characteristic time. Lippens *et al.* [6, 7] found in oriented samples aligned perpendicularly to the electric field, a low frequency process that they attributed to molecular associations resulting from the existence of short range forces. Cramer *et al.* [20] assign a low frequency process in confined 5CB to partially immobilized molecules in a surface layer with a temperature dependence that follows the behaviour of the rotation about the short axis and the librational mode. Thus, it seems reasonable to relate our low frequency process to cooperative reorientations of molecular aggregates. In our case the mechanism has a temperature dependence close to the one observed in the other two processes. However, at the lowest temperatures studied, the loss peak position remains unchanged, probably because the architecture of these molecular domains no longer varies (although an exchange between immobilized and free molecules is allowed). Nevertheless some care

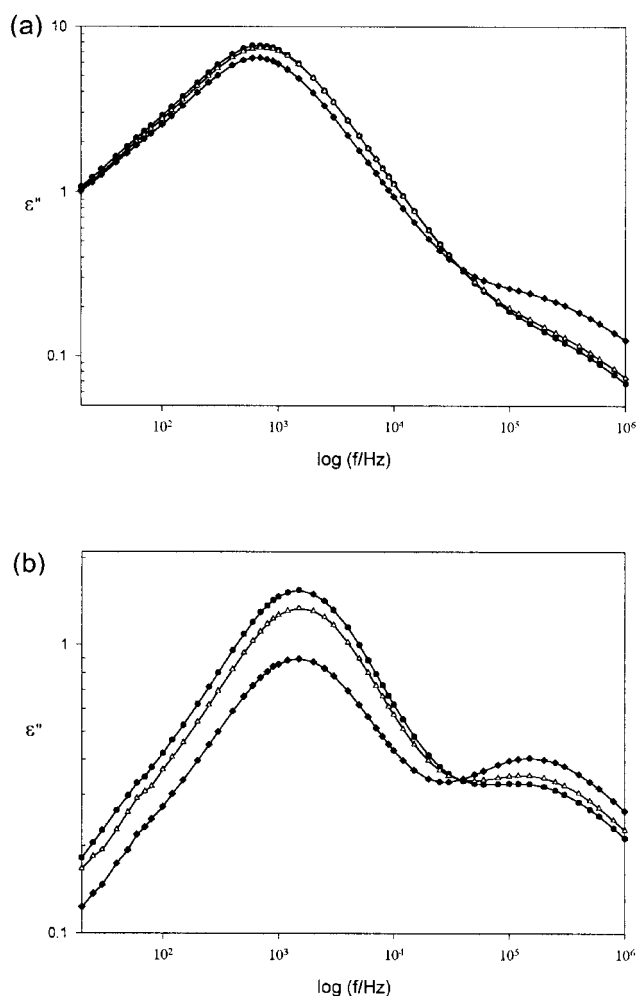


Figure 9. Dielectric loss curves on a logarithmic scale for (a) bulk E7 and (b) HPC + E7 at 237 K. Filled circles: normal cooled method; open triangles: 30 min at 237 K after the fast cooling; filled diamonds: fast cooling method.

must be taken in the interpretation of the results related to this low frequency mechanism, since it is largely merged in the main peak.

3.4. The Maxwell-Wagner (MW) effect

The possibility of changing the state of a liquid crystal composite from opaque to transparent is one of the most interesting and useful applications of these classes of material, namely in smart window applications [33]. The transparent state is reached through the application of an electric field applied by transparent electrodes on each side of the composite system, orientating the liquid crystal domains in such a way that the refractive index of the liquid crystal matches the refractive index of the polymer. The conditions for aligning the liquid crystal may be influenced by different factors such as surface alignment [34], the dielectric constant of the polymer

film, the liquid crystal–polymer surface interactions as we mentioned before [32], and the Maxwell-Wagner effect.

As we observed in figure 3 for the HPC + E7 system, the loss curves at low frequencies and for the higher temperatures show an abnormal increase that we attributed to the MW effect. When this effect appears, the curves of the real permittivity increase in the low frequency region. In figure 10 we present the ϵ' curves for the composite system where this effect is visible.

The MW effect is due to the coexistence of two media of different dielectric constant, where a charge build-up occurs in the polymer–liquid crystal interface. As Zhong *et al.* [15] pointed out, it plays a crucial role in the electro-optic properties of the composite film, and may determine the driving frequency and voltage. The interfacial charges may screen the liquid crystal molecules from coupling with the external field, and a higher voltage and frequency could be necessary to align the liquid crystal director parallel to the field. This effect depends also on the temperature, being present to some extent even at room temperature and at frequencies lower than 100 Hz. In consequence, care has to be taken to optimize the variables frequency and voltage, in order to switch the composite film from a scattering state to a transparent state.

4. Conclusions

By studying the unaligned mixture E7 in the super-cooled state, it was possible to bring into our frequency range (20 Hz–1 MHz) the relaxation processes usually observed in the nematic state in the megahertz and low gigahertz frequency regions. The typical behaviour found

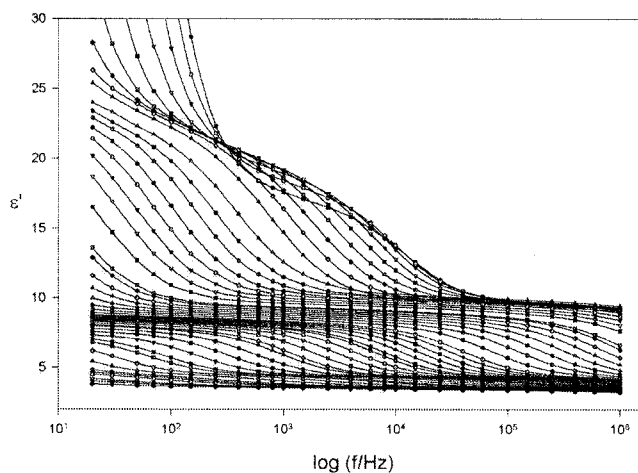


Figure 10. Real permittivity of HPC + E7 as a function of frequency within the temperature range 213 to 373 K, showing the Maxwell-Wagner effect.

in oriented samples, with the director aligned either parallel or normal to the electric field, is found simultaneously in this unaligned sample. Therefore, the dielectric spectra present the superposition of three different relaxation mechanisms: a low frequency non-Debye process whose quantitative analysis is difficult, but that could be related to molecular aggregates (related to the perpendicular alignment of the director in the electric field in an oriented sample); a main relaxation peak of Debye type involving the hindered rotation about the short molecular axis (related to the parallel alignment of the director in the electric field); and a high frequency non-Debye process related to the tumbling of molecules (related again to the perpendicular alignment of the director in the electric field as is the case in an oriented sample). Although the three relaxation processes are still present in the composite system, the high frequency process is greatly favoured when the liquid crystal rests on the hydroxypropylcellulose substrate; this indicates an increase, relative to pure E7, of the number of dipoles with a component of the dipole moment vector along the perpendicular direction in the electric field, which may be attributed to surface effects. All three relaxation mechanisms are temperature dependent, although the low frequency process seems to be temperature independent at the lowest temperatures. The temperature dependence of the main relaxation process, in pure E7 and in HPC + E7, follows VFT behaviour; also observed in confined nematics at temperatures well below the crystallization temperature, confirming that this temperature dependence is an intrinsic property of the supercooled state as is observed in glass-forming liquids. The high frequency process seems to have a temperature dependence close to the main process presenting also some curvature in the activation plot. The relaxation time of the main process increases when the liquid crystal mixture rests on the hydroxypropylcellulose film, with the maximum in dielectric loss located 0.3 decade higher in the frequency window (or 3–4 K lower in a temperature window) relative to pure E7.

For both systems there is a temperature below which the values of both $\Delta\epsilon$ and ϵ''_{\max} of the main peak decrease abruptly. The relative intensities of the main and secondary peaks of the dielectric spectra for temperatures close to and below that temperature, become strongly cooling rate dependent. This behaviour seems to indicate the presence of a transition (also detected by DSC, but fairly reproducible); more work is in progress to clarify the origin of this transition.

Due to the Maxwell-Wagner effect in HPC + E7, special care has to be taken in order to optimize both frequency and voltage to switch the composite film from a scattering state to a transparent state.

This work was supported by Fundação para a Ciência e Tecnologia through the project PRAXIS/QUI/10071/98. The authors wish to thank Prof. J. L. Figueirinhas for helpful discussions and critical reading of the manuscript.

References

- [1] GODINHO, M. H., FIGUEIRINHAS, J. L., and MARTINS, A. F., 1996, *Liq. Cryst.*, **20**, 373.
- [2] GODINHO, M. H., FIGUEIRINHAS, J. L., ALMEIDA, A., and MARTINS, A. F., 1997, in Proceedings of the 5th European Conference on Advanced Materials, Processes and Applications; Material, Functionality and Design (Polymer and Ceramics), Vol. II. p. II–111.
- [3] GODINHO, M. H., COSTA, C., and FIGUEIRINHAS, J. L., 1999, *Mol. Cryst. liq. Cryst.*, **173**, 331.
- [4] GODINHO, M. H., and FIGUEIRINHAS, J. L., private communication.
- [5] DAVIES, M., MOUTRAN, R., PRICE, A. H., BEEVERS, M. S., and WILLIAMS, G., 1976, *J. chem. Soc. Faraday Trans. II*, **72**, 1447.
- [6] LIPPENS, D., PARNEIX, J. P., and CHAPOTON, A., 1977, *J. Physique*, **38**, 1465.
- [7] WACRENIER, J. M., DRUON, C., and LIPPENS, D., 1981, *Mol. Phys.*, **43**, 97.
- [8] BUKA, A., OWEN, P. G., and PRICE, A. H., 1979, *Mol. Cryst. liq. Cryst.*, **51**, 273.
- [9] MURTHY, U. M. S., and VIJ, J. K., 1989, *J. chem. Phys.*, **90**, 1974.
- [10] DRUON, C., and WACRENIER, J. M., 1977, *J. Physique*, **38**, 47.
- [11] MARTIN, A. J., MEIER, G., and SAUPE, A., 1971, *Symp. Faraday Soc.*, **5**, 119.
- [12] BOSE, T. K., CHAHINE, R., MERABET, M., and THOEN, J., 1984, *J. Physique*, **45**, 1329.
- [13] BOSE, T. K., CAMPBELL, B., YAGIHARA, S., and THOEN, J., 1987, *Phys. Rev. A*, **36**, 5767.
- [14] KRESSE, H., 1983, *Advances in Liquid Crystals*, Vol. VI edited by G. H. Brown (New York: Academic Press).
- [15] ZHONG, Z. Z., SCHUELE, D. E., GORDON, W. L., ADAMIC, K. J., and AKINS, R. B., 1992, *J. polym. Sci. B: polym. Phys.*, **30**, 1443.
- [16] HASEGAWA, R., SAKAMOTO, M., and SASAKI, H., 1993, *Appl. Spectrosc.*, **47**, 1386.
- [17] HAVRILIAK, S., and NEGAMI, S., 1966, *J. polym. Sci. C*, **14**, 99.
- [18] ROUSSEL, F., BUISINE, J. M., MASCHKE, U., and COQUERET, X., 1998, *Liq. Cryst.*, **24**, 555.
- [19] ROUSSEL, F., MASCHKE, U., COQUERET, X., and BUISINE, J. M., 1998, *C. R. Acad. Sci. Paris*, **326**, Série II b, 449.
- [20] CRAMER, C. H., CRAMER, T. H., KREMER, F., and STANNARIUS, R., 1997, *J. chem. Phys.*, **106**, 3730.
- [21] SINHA, G. P., and ALIEV, F. M., 1988, *Phys. Rev. E*, **58**, 2001.
- [22] ZELLER, H. R., 1982, *Phys. Rev. Lett.*, **48**, 334.
- [23] NAZARIO, Z., SINHA, G. P., and ALIEV, F. M., *Mol. Cryst. Liq. Cryst.* (to be published).
- [24] ZELLER, H. R., 1981, *Phys. Rev. A*, **23**, 1434.
- [25] WERNER, J., OTTO, K., ENKE, D., PELZIL, G., JANOWSKI, F. A., and KRESSE, H., 2000, *Liq. Cryst.*, **27**, 1295.
- [26] STILLINGER, F. H., and WEBER, T. A., 1983, *Phys. Rev. A*, **28**, 2408.

- [27] SCHRÖDER, T. B., SASTRY, S., DYRE, J. C., and GLOTZER, S. C., 2000, *J. chem. Phys.*, **112**, 9834.
- [28] ZAKHAROV, A. V., and DONG, R. Y., 2000, *Phys. Rev. E*, **63**, 011704.
- [29] SCHADT, M., 1972, *J. chem. Phys.*, **56**, 1494.
- [30] SCHÖNHALS, A., ZOBOWA, H. L., FRICKE, R., FRUNZA, S., FRUNZA, L., and MOLDOVAN, R., 1999, *Cryst. Res. Technol.*, **34**, 1309.
- [31] MANAILA-MAXIMEAN, D., FURLANI, M., BENA, R., STOIAN, V., and ROSU, C., 2000, *Proc. SPIE*, **4068**, 45.
- [32] ALMEIDA, P. L., GODINHO, M. H., CIDADE, M. T., and FIGUEIRINHAS, J. L., *Mol. Cryst. Liq. Cryst.* (to be published).
- [33] BOUTELLER, L., and LE BARNY, P., 1996, *Liq. Cryst.*, **21**, 157.
- [34] CLARK, M. G., 1979, *Displays*, 17.